

## Rhenium Uptake as Analogue for $^{99}\text{Tc}$ by Steel Corrosion Products

Kenneth M. Krupka,\* Christopher F. Brown, H. Todd Schaeff, Steve M. Heald, Michelle M. Valenta, and Bruce W. Arey

*Pacific Northwest National Laboratory, P.O. Box 999, Richland, Washington 99352*

*\*E-mail: ken.krupka@pnl.gov*

**Abstract** – *Static batch experiments were used to examine the sorption of dissolved perrhenate [Re(VII)], as a surrogate for pertechnetate [Tc(VII)], on corrosion products of A-516 carbon steel coupons contacted with synthetic groundwater or dilute water. After 109 days of contact time, the concentration of dissolved Re(VII) in the synthetic groundwater matrix decreased by approximately 26%; the dilute water matrix experienced a 99% decrease in dissolved Re(VII) over the same time period. Bulk x-ray diffraction (XRD) results for the corroded steel coupons showed that the corrosion products consisted primarily of maghemite, lepidocrocite, and goethite. Analyses of the coupons by scanning electron microscopy/energy dispersive spectroscopy (SEM/EDS) indicated that Re was present with the morphologically complex assemblages of Fe oxide/hydroxide corrosion products for samples spiked with the highest dissolved Re(VII) concentration (1.0 mmol/L) used for these experiments. Analyses of corroded steel coupons contacted with solutions containing 1.0 mmol/L Re(VII) by synchrotron-based methods confirmed the presence of Re sorbed with the corrosion product on the steel coupons. Analyses showed that the Re sorbed on these corroded coupons was in the +7 oxidation state, suggesting that the Re(VII) uptake mechanism did not involve reduction of Re to a lower oxidation state, such as +4. The results of our studies using Re(VII) as an analogue for  $^{99}\text{Tc(VII)}$  suggest that  $^{99}\text{Tc(VII)}$  would also be sorbed with steel corrosion products and that the inventory of  $^{99}\text{Tc(VII)}$  released from breached waste packages would be lower than what is now conservatively estimated.*

### I. INTRODUCTION

The Office of Civilian Radioactive Waste Management (OCRWM) in the U.S Department of Energy (DOE) is responsible for developing a federal system to dispose of spent nuclear fuel from commercial nuclear reactors. For two decades, the OCRWM has studied Yucca Mountain in Nevada to determine its suitability as a geological repository for high-level nuclear waste. Current performance assessments predict that if waste packages containing spent nuclear fuel are breached,  $^{99}\text{Tc}$  will be one of the primary isotopes critical to the predicted dose for the health and safety performance of the Yucca Mountain Site over the first 50,000 years. Dose was treated conservatively in the total system performance assessment supporting the 2002 site recommendation, and the conditions associated with the surrounding corrosion product in waste packages were conservatively assumed to retain ambient oxidizing conditions [1]. Moreover, uptake of  $^{99}\text{Tc}$  onto corroding waste packages was not included.

Reduction of redox-sensitive radionuclides, such as  $^{99}\text{Tc}$ , can occur by surface-mediated, heterogeneous reduction/sorption reactions on Fe(0)- or Fe(II)-

containing solids. The surface-mediated heterogeneous reduction of Tc(VII) to Tc(IV) by electron transfer from Fe(II)-containing minerals has been studied [2,3,4]. However, this process has not been studied with respect to uptake of Tc(VII) by Fe oxides as they form during corrosion of metals under oxic conditions. For Tc, this process involves a series of electron transfer reactions resulting in the 1) oxidation of Fe(0) or Fe(II) to Fe(III) and the ensuing formation of Fe(III)-oxide surface coatings, and 2) the reduction of highly mobile Tc(VII) to a less soluble, lower valence state [Tc(IV)]. Under most pH conditions, the solubility of the Tc(IV) species is so low that Tc precipitates as either sparingly soluble, amorphous  $\text{TcO}_2 \cdot n\text{H}_2\text{O}$  and/or possibly as a mixed Tc(IV)/Fe(III) oxide co-precipitate. Due to the thermodynamic stability of Fe(III) oxides, some co-precipitation of Tc as a mixed Tc(IV)/Fe(III) oxide may be irreversible in waste package and environmental systems.

The overall objective of our research is to characterize the reactions that affect the sequestration and release of  $^{99}\text{Tc}$  by Fe oxide/hydroxide solids that precipitate during corrosion of Fe-based materials used in the waste package, such as A-516 carbon steel used in the fuel basket. Initial testing was completed using solutions

spiked with perrhenate [Re(VII)] as a surrogate for pertechnetate [Tc(VII)]. Rhenium is considered an analogue for Tc due to the similarities of their chemistries. The first ionization potentials and atomic radii for Re and Tc are similar, and +7 and +4 are their most stable oxidation states. In oxic aqueous systems,  $\text{ReO}_4^-$  and  $\text{TcO}_4^-$  are their predominant ionic forms, which as anions, are very mobile in most environmental systems. The Re(VII)-spiked experiments were completed first to refine test procedures, sample preparation, and analysis methods without restrictions from handling radioactive materials or the added costs of radioactive waste disposal.  $^{99}\text{Tc(VII)}$ -spiked experiments and characterization studies similar to those described below are currently in progress.

Results from our studies will provide information about the mechanism(s) that control the uptake and extent of reversibility of  $^{99}\text{Tc}$  sorption<sup>1</sup> onto and off steel corrosion products. This information is essential to understanding the fate of  $^{99}\text{Tc}$  in the repository environment. This in turn will allow the development of less pessimistic models for the prediction of the nominal dose contributions from  $^{99}\text{Tc}$ .

## II. EXPERIMENTAL DETAILS

Batch reaction experiments at room temperature under oxic conditions were completed to examine the sorption of dissolved Re(VII) on corrosion products of A-516 carbon steel coupons reacted with synthetic J-13 groundwater<sup>2</sup> or dilute (tap) water spiked with 0, 0.001 (0.186 ppm), and 1.0 mmol/L ( $1.86 \times 10^{-4}$  ppm) dissolved Re(VII). The composition of the synthetic J-13 groundwater approximates that of water from supply well No. J-13 near Yucca Mountain. The composition of water from well No. J-13 (Table I) [5] is a dilute Na-HCO<sub>3</sub>-CO<sub>3</sub> groundwater which is considered a possible proxy for the composition of perched waters at Yucca Mountain [5,6,7]. Dilute (tap) water (Table I) was used for initial testing to represent the other limit in the range of compositions for water that might intrude and react with the waste package.

Test vials were sampled after 30 and 109 days, and the resulting solutions and reacted coupons were removed for analysis and characterization. The solution samples were analyzed for pH, major cations and some trace metals by inductively coupled plasma-atomic emission

<sup>1</sup> Throughout this manuscript, “sorption” will be used as a generic term devoid of mechanism when it is not possible to determine indisputably if the uptake mechanism is surface adsorption and/or co-precipitation (i.e., structural absorption).

<sup>2</sup> Recipe for the synthetic J-13 groundwater provided by James L. Krumhansl (Sandia National Laboratories, Albuquerque, NM).

spectrometry (ICP-AES), and trace metals and Re by inductively coupled plasma-mass spectrometry (ICP-MS).

TABLE I.

Compositions for Water from Supply Well No. J-13 near Yucca Mountain [5] and Laboratory Dilute (Tap) Water

	J-13 Well Water	Dilute (Tap) Water
pH	7.41	7.43
	----- (mg/L) -----	
Na <sup>+</sup>	45.8	2.37
K <sup>+</sup>	5.04	0.561
Ca <sup>2+</sup>	13.0	19.8
Mg <sup>2+</sup>	2.01	4.18
SiO <sub>2</sub> (aq)	61.0	4.04
Cl <sup>-</sup>	7.14	3.32
SO <sub>4</sub> <sup>2-</sup>	18.4	9.61
HCO <sub>3</sub> <sup>-</sup>	129	NM <sup>1</sup>
NO <sub>3</sub> <sup>-</sup>	8.78	0.48
F <sup>-</sup>	2.18	ND <sup>2</sup>

<sup>1</sup> NM – Indicates the analyte was not measured.

<sup>2</sup> ND – Indicates the analyte was not detected or less than the quantification limit of the instrument.

The corroded steel coupons were rinsed several times with their respective Re-free starting solutions prior to storage and characterization. The corroded steel coupons and solids filtered from 30- and 109-day solution samples were characterized by x-ray diffraction (XRD) and scanning electron microscopy (SEM) in conjunction with energy dispersive spectroscopy (EDS) to identify the Fe corrosion products and extent of sorbed Re. Standard bulk powder XRD techniques were used to identify the crystalline phases present in corrosion product samples. Each sample was analyzed using a Scintag XRD unit equipped with a Peltier thermoelectrically-cooled detector and a copper x-ray tube. The diffractometer was operated at 45 kV and 40 mA. XRD scans were collected electronically and processed using the JADE<sup>®</sup> XRD pattern-processing software. Crystalline phases were identified by comparison of the background-subtracted XRD patterns for the corrosion product samples to the powder diffraction files (PDF<sup>™</sup>) published by the Joint Committee on Powder Diffraction Standards (JCPDS) International Center for Diffraction Data (ICDD).

A JEOL JSM 840 SEM was used for high-resolution imaging of the morphologies and compositions of phases present on corroded steel coupons and in the

solids filtered from solution samples. The SEM system is equipped with an Oxford INCA EDS software system for semi-quantitative element analysis. Operating conditions for the SEM/EDS analyses consisted of 10 to 20 keV for SEM imaging, and 20 to 30 keV, 100 live seconds for the EDS analyses.

Synchrotron-based<sup>3</sup> x-ray techniques, including x-ray microfluorescence ( $\mu$ XRF), x-ray absorption spectroscopy (XAS), and x-ray microdiffraction ( $\mu$ XRD), were also used to characterize the surfaces of corroded coupons and determine the oxidation state and speciation of Re sorbed to the corrosion products. Steel coupons provided for study included a pristine A-516 coupon and coupons that were reacted with synthetic groundwater or dilute water containing 1.0 mmol/L dissolved Re(VII). Samples of reagent-grade solid  $\text{ReO}_2$ ,  $\text{KReO}_4$ , and  $\text{NaReO}_4$  were used as Re(IV) and Re(VII) standards for XAS analyses. Prior to their use, the identification of the Re solid present in each standard was confirmed by bulk XRD. Initial analyses began with bulk extended x-ray absorption fine structure (EXAFS) scans using the bending magnet beam line 20-BM [8]. These scans averaged over an area of  $1 \times 10$  mm near the center of the coupons. For good statistics, several scans were run for each sample and later averaged. Subsequent  $\mu$ XRF, XAS, and  $\mu$ XRD analyses were completed using the insertion device beamline 20-ID [8,9] where the incident x-ray microbeam was focused to a spot size of about 2  $\mu\text{m}$  using a pair of Kirkpatrick-Baez mirrors. To allow for diffraction measurements, the samples were oriented at an angle of  $12^\circ$  with respect to the incident beam. This gave an effective resolution of 10  $\mu\text{m}$  horizontally. For both beamlines, the x-rays are monochromatized using a Si(111) double-crystal monochromator with an energy resolution of about 1.5 eV. A  $\text{KReO}_4$  standard was used to monitor the energy calibration. A multi-element Ge detector was used to detect the x-ray fluorescence from Re and other elements of interest. After the  $\mu$ XRF scans were completed, locations of interest were selected for further analysis by XAS. The x-ray absorption near edge structure (XANES) and EXAFS were examined to determine the oxidation state and the speciation of sorbed Re based on its coordination. These XANES and EXAFS data were analyzed using the IFEFFIT suite of analysis programs [10]. Several locations on the two corroded coupons were also studied by  $\mu$ XRD.

<sup>3</sup> The synchrotron-based analyses were completed on the Advanced Photon Source (APS) beamlines 20-BM and 20-ID (PNC-CAT) [8,9] at the Argonne National Laboratory (Argonne, IL).

### III. RESULTS

Analyses of solution samples (Table II) from the Re uptake experiments indicated that the concentrations of dissolved Re, Ca, and Si for all experiments completed in both solution matrices decreased from 0 to 109 days. After 109 days, the concentrations of dissolved Si in all solution samples were less than the analytical detection limit.

Bulk XRD results for the filter samples and corroded steel coupons reacted for 30 and 109 days showed that the corrosion products consisted primarily of maghemite ( $\gamma\text{-Fe}_2\text{O}_3$ ), lepidocrocite [ $\gamma\text{-FeO(OH)}$ ], and goethite [ $\alpha\text{-FeO(OH)}$ ]. Magnetite ( $\text{Fe}_3\text{O}_4$ ) was also identified on coupons reacted for 109 days in the Re(VII)-spiked simulated J-13 groundwater. Fig. 1 shows the background-subtracted XRD patterns measured with  $\text{CuK}\alpha$  radiation ( $\lambda=1.5406 \text{ \AA}$ ) for filterable corrosion product samples from the 30-day open-vial experiments with A-516 carbon steel coupons in contact with 1.0 mM Re(VII)-spiked synthetic J-13 or dilute waters. The XRD patterns are shown for comparison purposes along with the schematic database patterns for goethite [ $\text{FeO(OH)}$ ] (PDF #29-0713), maghemite ( $\text{Fe}_2\text{O}_3$ ) (PDF #39-1346), and lepidocrocite [ $\text{FeO(OH)}$ ] (PDF #08-0098) at bottom of Fig. 1. The relative proportions of these Fe

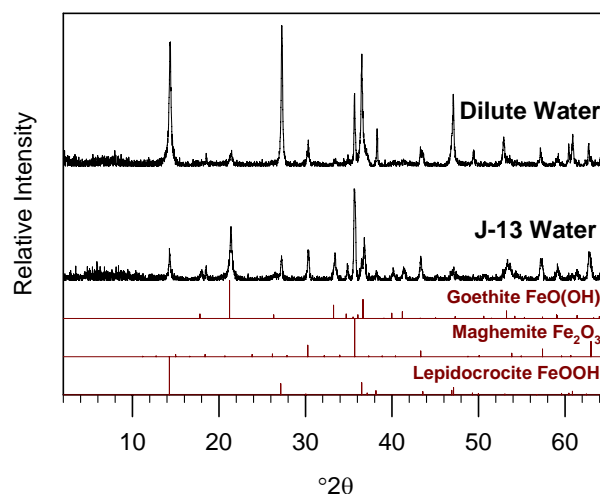


Fig. 1. XRD patterns measured with  $\text{CuK}\alpha$  radiation ( $\lambda=1.5406 \text{ \AA}$ ) for filterable corrosion product samples from the 30-day experiments with A-516 carbon steel coupons in contact with 1.0 mmol/L Re(VII)-spiked dilute (top) and synthetic J-13 waters (second from top).

TABLE II

Analyses of pH and Dissolved Re, Ca, and Si in Solution Samples at 0, 30, and 109 Days

Type of Solution	Initial Re(VII) Spike (mmol/L)	Time (days)	pH	Re <sup>1</sup>	Ca	Si
				----- $\mu\text{g/L}$ -----		
Dilute Water	0.001	0	7.62 $\pm$ 0.10	177 $\pm$ 1.95 <sup>2</sup>	19,900 $\pm$ 214	1,860 $\pm$ 12.0
		30	6.63 $\pm$ 0.10	0.532 $\pm$ 0.028	2,930 $\pm$ 105	ND <sup>3</sup>
		109	6.08 $\pm$ 0.10	0.959 $\pm$ 0.043	1,560 $\pm$ 85.7	ND
	1.0	0	7.58 $\pm$ 0.10	189,000 $\pm$ 756	20,600 $\pm$ 489	1,770 $\pm$ 4.32
		30	6.97 $\pm$ 0.10	121,000 $\pm$ 1201	3,166 $\pm$ 113	ND
		109	7.16 $\pm$ 0.10	1,730 $\pm$ 93.7	480 $\pm$ 65.9	ND
J-13 Water	0.001	0	8.78 $\pm$ 0.10	186 $\pm$ 0.744	2,820 $\pm$ 7.90	12,900 $\pm$ 4.72
		30	8.04 $\pm$ 0.10	33.8 $\pm$ 0.237	1,710 $\pm$ 68.5	ND
		109	8.81 $\pm$ 0.10	7.61 $\pm$ 0.134	ND	ND
	1.0	0	8.70 $\pm$ 0.10	187,000 $\pm$ 2340	2,400 $\pm$ 52.0	13,000 $\pm$ 85.3
		30	7.90 $\pm$ 0.10	163,000 $\pm$ 1060	1,510 $\pm$ 80.2	ND
		109	9.00 $\pm$ 0.10	139,000 $\pm$ 1250	ND	ND

<sup>1</sup> Concentrations of Re are reported as total Re and are the average of the values from the ICP-MS analyses of <sup>185</sup>Re and <sup>187</sup>Re.

<sup>2</sup> Uncertainties listed for concentrations of dissolved Re, Ca, and Si are one standard deviation for the three replicate analyses made for each solution sample. Uncertainties listed for pH measurements are based on the measurement procedure and pH standards.

<sup>3</sup> ND - Indicates the analyte was not detected or less than the quantification limit of the instrument.

oxide/hydroxide phases differed slightly for different experimental conditions and between the filter versus coupon samples. The XRD analysis of corrosion products in the filter and steel-coupon samples did not identify any solids containing Re, Ca, or Si.

Analyses of the corroded steel coupons by SEM/EDS indicated that the corrosion products on the steel coupons reacted in synthetic groundwater or dilute waters at 30 and 109 days consisted of morphologically complex assemblages of Fe oxide/hydroxide solids. Fig. 2 shows SEM secondary-electron micrographs of a pristine A-516 carbon steel coupon (Fig. 2A) and of typical morphologies of Fe oxide/hydroxide solids that precipitated on the corroded steel coupons (Fig. 2B to 2F). Analyses in progress by  $\mu$ XRD will help identify the specific Fe oxide/hydroxide phases that form the different morphologies of corrosion products observed by SEM.

The EDS analyses of the corroded coupons reacted for 30 and 109 days showed that Re was present with the corrosion products for solutions spiked with 1.0 mmol/L Re(VII). Fig. 3 shows a typical EDS spectrum for an area on a steel coupon that was reacted in synthetic J-13

groundwater spiked with 1.0 mmol/L Re(VII). The Re concentration calculated by the Oxford INCA EDS software system for the EDS spectra shown in Fig. 3 is about 8 wt.%. For five EDS analyses collected in different locations in the sample area shown in Fig. 3, the calculated Re concentrations range from approximately 3 to 8 wt.%. Similar EDS results were obtained for the coupons reacted for 30 and 109 days with dilute water spiked with 1.0 mmol/L Re(VII). Because the reacted coupons were rinsed several times with their respective Re-free starting solutions prior to storage and SEM/EDS analysis, the Re associated with the corrosion products is likely not surface adsorbed and is currently assumed to be co-precipitated with the corrosion products. EDS analyses did not detect sorption of Re by corrosion products that precipitated on steel coupons reacted in solutions spiked with 0.001 mmol/L Re(VII). Because ICP-MS analyses showed that the concentrations of dissolved Re in the 30- and 109-day synthetic groundwater and dilute water samples decreased from their initial concentrations of 0.001 mmol/L, Re uptake occurred but the concentrations of Re sorbed in corrosion products from the experiments spiked with 0.001 mmol/L Re(VII) were likely too low to be detected by EDS.

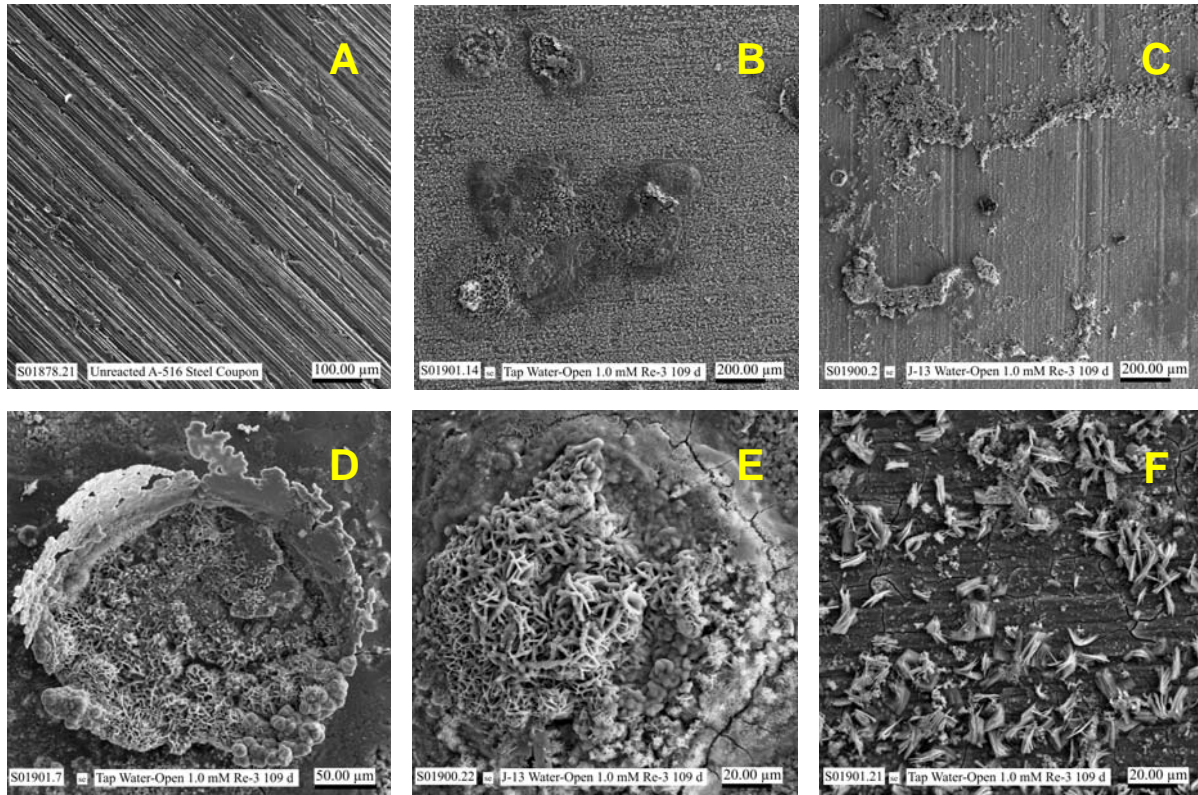


Fig. 2. SEM micrographs of a pristine A-516 carbon steel coupon (micrograph A) and typical morphologies of corrosion product (micrographs B through F) on coupons reacted for 109 days in contact with 1.0 mmol/L Re(VII)-spiked synthetic J-13 (micrographs C and E) or dilute waters (micrographs B, D, and F).

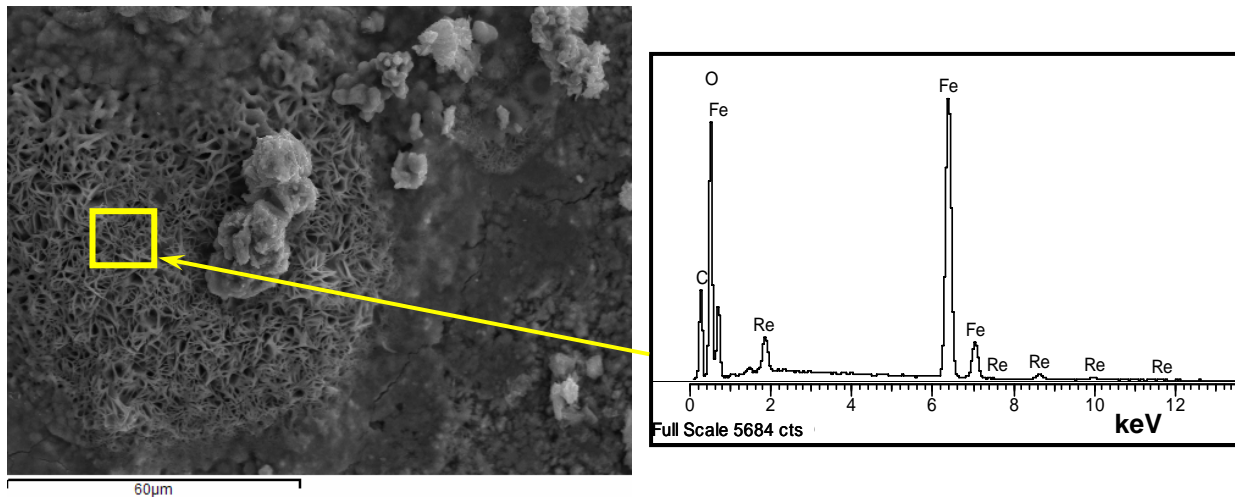


Fig. 3. SEM/EDS analysis showing uptake of Re by corrosion product on an A-516 carbon steel coupon reacted for 109 days in contact with 1.0 mmol/L Re(VII)-spiked synthetic J-13 groundwater.

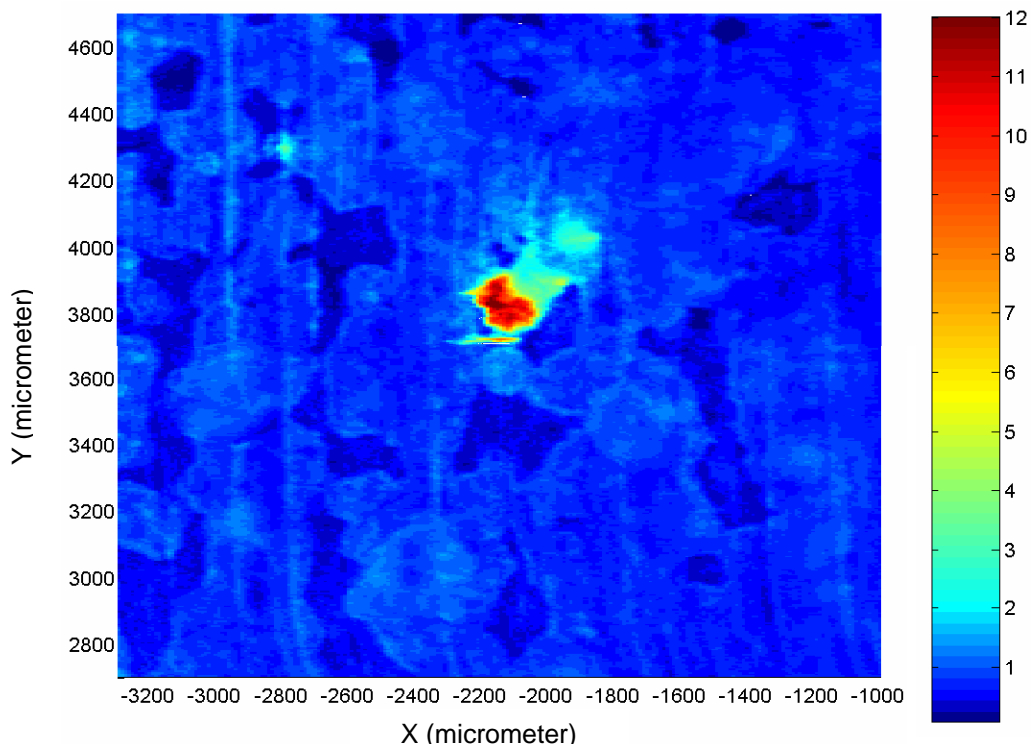


Fig. 4.  $\mu$ XRF map for Re on corroded coupon reacted in synthetic J-13 groundwater spiked with 1.0 mmol/L Re(VII). [The scale bar on right shows the relative concentrations of Re.]

Analyses of corroded steel coupons reacted with solutions spiked with 1.0 mmol/L Re(VII) by synchrotron-based methods confirmed the uptake of Re by the corroded coupons as determined by SEM/EDS. The synchrotron-based micro-analyses identified localized regions that were highly enriched with sorbed Re relative to other regions of corrosion product (Fig. 4), and showed that all Re, regardless of enrichment, was sorbed in the +7 oxidation state consistent with the first neighbor bonding for  $\text{ReO}_4^-$ . Fig. 5 shows the merged, normalized Re  $L_{\text{III}}$ -edge XANES spectra measured on the bending magnet beam line for corroded coupons reacted in synthetic J-13 or dilute waters compared to the spectra for the Re standards. The XANES spectra measured on the bending magnet (Fig. 5) and insertion device beamlines were consistent with the spectra for Re(VII) standards  $\text{KReO}_4$  and  $\text{NaReO}_4$  but not the Re(IV) standard  $\text{ReO}_2$ . Fig. 6 illustrates the merged Re  $L_{\text{III}}$ -edge EXAFS spectra from the bending magnet beam line analyses for corroded coupons reacted in synthetic J-13 or dilute waters. These data are weighted by  $k^2$  to emphasize the high  $k$  signal. The spectra in Fig. 6 demonstrate that near neighbor bonding is essentially identical to that of the  $\text{ReO}_4^-$  ion in  $\text{KReO}_4$  and not that of Re(IV) in  $\text{ReO}_2$ . The  $\text{ReO}_4^-$  ion remains intact upon incorporation into the corrosion product.

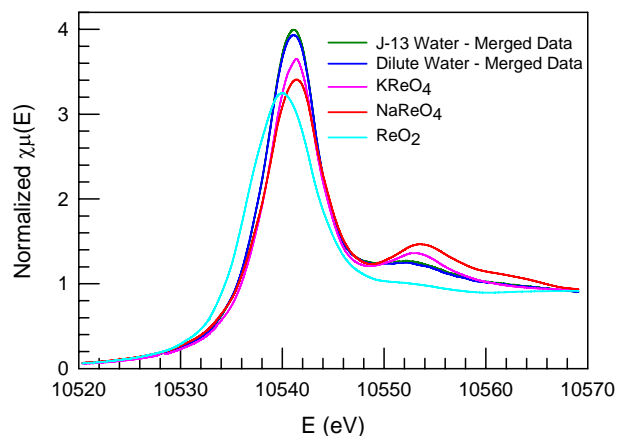


Fig. 5 Merged, normalized Re  $L_{\text{III}}$ -edge XANES spectra measured on the bending magnet beam line for corroded coupons reacted in synthetic J-13 or dilute waters compared to the spectra for the Re standards.

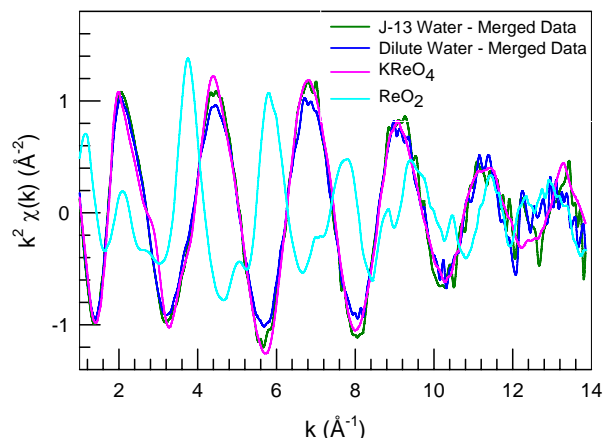


Fig. 6 Merged Re  $L_{III}$ -edge EXAFS spectra measured on the bending magnet beam line for corroded coupons reacted in synthetic J-13 or dilute waters compared to the spectra for the Re standards.

#### IV. CONCLUSIONS

The results of these studies indicate that Re(VII) can be sorbed with Fe oxides/hydroxides that precipitate during the corrosion of steel. The Re sorbed on these corroded coupons is in the +7 oxidation state, which suggests that the Re(VII) uptake mechanism does not involve reduction of Re from +7 to a lower oxidation state such as +4 as originally hypothesized. Regardless of the mechanism responsible for the observed Re sorption, our results using Re(VII) as an analogue for  $^{99}\text{Tc(VII)}$  suggest that  $^{99}\text{Tc(VII)}$  would also be sorbed with steel corrosion products and that the inventory of  $^{99}\text{Tc}$  released from breached waste packages would be lower than what is now conservatively estimated.

As noted previously,  $^{99}\text{Tc(VII)}$ -spiked experiments and characterization studies similar to those described in this paper are currently in progress. Except for the extent of corrosion and oxidation state of the sorbed  $^{99}\text{Tc}$ , the results from 30-day  $^{99}\text{Tc(VII)}$ -spiked experiments obtained to date (manuscript in progress) are consistent with the Re results (i.e., measured uptake of  $^{99}\text{Tc}$  by corrosion product) described above. However, in  $^{99}\text{Tc(VII)}$ -spiked experiments, less corrosion product is observed on the A-516 carbon steel coupons and, based on the XANES and EXAFS analyses, approximately 80 to 100% of  $^{99}\text{Tc}$  sorbed to Fe oxides/hydroxides is in the +4 oxidation state depending on the type of water. These results suggest that the standard potential for the Re(VII)/Re(IV) may be significantly lower than that for Tc(VII)/Tc(IV) and thus Re may not be an adequate surrogate for studying the geochemical behavior of  $^{99}\text{Tc}$  at environmentally relevant reducing conditions.

#### ACKNOWLEDGMENTS

The authors are particularly grateful for the technical reviews and helpful comments provided by K. J. Cantrell (PNNL) and the anonymous reviewers of the proceedings papers. The authors would also like to thank S. R. Baum, E. T. Clayton, and K. N. Geiszler (all of PNNL) for completing the chemical analyses of the solution samples from our studies. The Pacific Northwest National Laboratory (PNNL) is operated by Battelle for the DOE under Contract DE-AC05-76RLO 1830. This study has been funded in whole or in part by the DOE OCRWM Office of Science and Technology and International. Use of the Advanced Photon Source (APS) is supported by the DOE Office of Science, Office of Basic Energy Sciences, under Contract No. W-31-109-Eng-38. The Pacific Northwest Consortium-Collaborative Access Team (PNC-CAT) beamlines are supported by funding from DOE Basic Energy Sciences, the University of Washington, Simon Fraser University, and the NSERC in Canada. The PNNL Quality Assurance program has been evaluated and approved by OCRWM OST&I. Therefore, the data qualification status of these Re experiments should be considered qualified, as specified by the latest revision of OCRWM procedure LP-SIII.2Q-BSC, *Qualification of Unqualified Data*.

#### REFERENCES

1. CRWMS M&O (Civilian Radioactive Waste Management System Management & Operating Contractor), "Total System Performance Assessment for the Site Recommendation," TDR-WIS-RL-000001 Rev 04 ICN 01: Bechtel SAIC Company LLC, Las Vegas, Nevada (2000).
2. D. CUI and T. E. ERIKSEN, "Reduction of Pertechnetate in Solution by Heterogeneous Electron Transfer from Fe(II) Containing Geological Material," *Environ. Sci. Technol.*, **30**, 2263 (1996).
3. R. I. HAINES, D. G. OWEN, and T. T. VANDERGRAAF, "Technetium-Iron Oxide Reactions Under Anaerobic Conditions: A Fourier Transform Infrared, FTIR Study," *Nucl. J. Canada*, **1**, 32 (1987).
4. T. T. VANDERGRAAF, K. V. TICKNOR, and I. M. GEORGE. "Reactions between Technetium in Solution and Iron-Containing Minerals Under Oxidic and Anoxic Conditions," In *Geochemical Behavior of Disposed Radioactive Waste*, G. S. Barney, J. D. Navratil, and W. W. Schulz (eds.), ACS Symposium Series 246, p. 25, American Chemical Society, Washington, D.C. (1984).
5. J. HARRAR, J. F. CARLEY, W. F. ISHERWOOD, and E. RABER, "Report of the Committee to Review the Use of J13 Well Water in Nevada Nuclear Waste

- Storage Investigations,” UCRL-ID-21867: Lawrence Livermore National Laboratory, Livermore, California (1990).
6. N. D. ROSENBERG, G. E. GDOWSKI, and K. G. KNAUSS, ”Evaporative Chemical Evolution of Natural Waters at Yucca Mountain, Nevada,” *Appl. Geochem.*, **16**, 1231 (2001).
  7. W. RUNDE, S. D. CONRADSON, D. W. EFURD, N. P. LU, C. E. VANPELT, and C. D. TAIT, ”Solubility and Sorption of Redox-Sensitive Radionuclides (Np, Pu) in J-13 Water from the Yucca Mountain Site: Comparison Between Experiments and Theory,” *Appl. Geochem.*, **17**, 837 (2002).
  8. S. M. HEALD, D. L. BREWE, E. A. STERN, K. H. KIM, F. C. BROWN, D. T. JIANG, E. D. CROZIER, and R. A. GORDON, ”XAFS and Micro-XAFS at the PNC-CAT Beamlines,” *J. Synchrotron Rad.*, **6**, 347 (1999).
  9. S. HEALD, E. STERN, D. BREWE, R. GORDON, D. CROZIER, D. JIANG, and J. CROSS, ”XAFS at the Pacific Northwest Consortium-Collaborative Access Team Undulator Beamline,” *J. Synchrotron Rad.*, **8**, Part 2, 342 (2001).
  10. B. RAVEL and M. NEWVILLE, ”ATHENA, ARTEMIS, HEPHAESTUS: Data Analysis for X-ray Absorption Spectroscopy Using IFEFFIT ,” *J. Synchrotron Rad.*, **12**, Part 4, 537 (2005).